Published in final edited form as:
Nat Neurosci. 2005 May ; 8(5): 650–656.

Fast Delayed Rectifier Potassium Current Required for Circadian Neural Activity

Itri JN[1], **Michel S**[1,2], **Vansteensel MJ**[2], **Meijer JH**[2], and **Colwell CS**[1]

[1]*Department of Psychiatry and Biobehavioral Sciences, University of California – Los Angeles, 760 Westwood Plaza, Los Angeles, California, 90024–1759* [2]*Department of Neurophysiology, Leiden University Medical Center, P.O. Box 9604, 2300 RC Leiden, The Netherlands*

Abstract

In mammals, the precise circadian timing of many biological processes depends on the generation of oscillations in neural activity of pacemaker cells in the suprachiasmatic nucleus (SCN). The ionic mechanisms underlying these rhythms are largely unknown. Using the mouse brain slice preparation, we demonstrate that the magnitude of fast delayed rectifier potassium currents exhibits a diurnal rhythm that peaks during the day. Importantly, this rhythm continues in constant darkness, providing the first demonstration of the circadian regulation of an intrinsic voltage–gated current in mammalian cells. Blocking this current prevented the daily rhythm in firing rate in SCN neurons. Kv3.1b and Kv3.2 potassium channels were found to be widely distributed within the SCN with higher expression during the day. We conclude that the fast delayed rectifier is necessary for the circadian modulation of electrical activity in SCN neurons, and represents an important part of the ionic basis for the generation of rhythmic output.

Keywords

circadian rhythms; Kv3.1b; potassium current; mouse; suprachiasmatic nucleus; SCN

Introduction

Almost all organisms, including humans, exhibit daily rhythms in their behavior and physiology. In most cases, endogenous cellular networks composed of multiple circadian oscillators generate these rhythms. These oscillators provide temporal structure to an organism's physiological systems. Nearly all behavioral processes show significant daily variations. This temporal variation plays an important role in the body's homeostatic mechanisms and has a major impact on the function of the nervous system. In mammals, the part of the nervous system responsible for most circadian behavior can be localized to a bilaterally paired structure in the hypothalamus known as the suprachiasmatic nucleus (SCN) [1]. Neurons in the SCN are intrinsic oscillators that continue to generate near 24-hour rhythms in electrical activity, secretion, and gene expression when isolated from the rest of the organism[2]. Previous studies suggest that a key component responsible for the generation of these rhythms is a molecular feedback loop that occurs in individual SCN neurons[3,4]. However, there is also evidence suggesting that membrane excitability and/or synaptic

Send correspondence to: CS Colwell, Department of Psychiatry, University of California – Los Angeles, 760 Westwood Plaza, Los Angeles, CA, 90024–1759 (U.S.A.), Telephone # (310) 206-3973, FAX (310) 206-5060, ccolwell@mednet.ucla.edu.

Competing interests statement
The authors declare that they have no competing financial interests.

transmission may be required for generation of the molecular oscillations[5,6]. Thus clarifying the ionic mechanisms interacting with the molecular feedback loop is critical to understanding the generation of circadian oscillations at both cellular and molecular levels of organization[7].

It is well accepted that voltage-dependent potassium (K^+) currents are primary regulators of membrane excitability[8]. Given their role in other neuronal systems, K^+ currents are likely candidates to couple clock-related gene expression to membrane excitability and spontaneous firing rate in the SCN. K^+ currents are a large and diverse family of voltage regulators and previous studies have characterized a number of intrinsic voltage gated K^+ currents in SCN neurons that are likely to play important roles in regulating the firing rate of SCN neurons[9–12]. However, the possibility of diurnal or circadian modulation of these K^+ currents has not been explored in any detail nor do we understand how selective currents regulate the daily rhythm in the frequency of action potentials in SCN neurons. We became interested in examining the possible circadian regulation of a subtype of K^+ currents known as the fast delayed rectifier (fDR) for two reasons. First, in molluskan retinal neurons, tetraethylammonium (TEA)-sensitive K^+ currents are thought to underlie the daily rhythm in electrical activity of these circadian pacemaker cells[13] and the slow delayed rectifier (sDR) current undergoes a circadian modulation[14]. Second, during the subjective day, SCN neurons exhibit sustained discharge for hours without spike adaptation and a variety of recent work suggest that the fDR current may allow for this type of discharge in other neurons[15,16]. In the present study, we found that the fDR currents are under circadian regulation and that these currents are critical for controlling the rhythm in firing rate that is characteristic of SCN neurons.

Results

Characterization of sDR and fDR currents

We used the whole-cell voltage-clamp technique to isolate and record K^+ currents from neurons in the mouse SCN. Each of these cells was determined to be within the SCN by directly visualizing the cell's location with IR–DIC videomicroscopy. In most cases, the IR-DIC images were sufficient to label a cell as being in either ventral or dorsal subregions[17]. Although these currents are present throughout the SCN, we focused on the dorsal subregion (dSCN) because this region exhibits more robust circadian rhythms in the transcription of clock-related genes and electrical activity[18,19].

Every SCN neuron exhibited sDR currents (n = 76). The sDR currents were isolated by subtraction ($I_{1\ mM\ TEA} - I_{20\ mM\ TEA}$, Fig. 1a) using a voltage step protocol [20,21] with a prepulse potential of −90 mV and test pulse potentials ranging from −80 to +50 mV (10 mV increments, Fig. 1a). The control artificial cerebral spinal fluid (ACSF) perfusion solution contained bicuculline (25 μM) to block $GABA_A$-mediated currents, TTX (0.5 μM) to block fast voltage-activated sodium channels, TEA (1 mM) or 4-aminopyridine (4–AP, 0.5 mM) to block fDR currents, and cadmium (100 μM) to block calcium (Ca^{2+}) channels. The treatment ACSF solution was identical to the control solution but with 20 mM TEA to block the sDR channels. The intracellular filling solution contained BAPTA (1 mM) to buffer intracellular Ca^{2+} and inhibit Ca^{2+}-dependent K^+ currents. The sDR currents in dSCN neurons showed an activation curve with a midpoint potential of 7.7 ± 0.4 mV and steep activation characteristics (slope factor k = 10.6 ± 0.5 mV, n = 7, Fig. 1b) during the day. The activation kinetics were similar during the night (midpoint 6.8 ± 0.6 mV, slope factor k = 9.9 ± 0.3 mV, n = 6, Fig. 1b). The 20–80% rise time was voltage-dependent in dSCN neurons (ranging from 57.1 ms at 10 mV to 4.6 ms at 50 mV, n = 11, Fig. 1c) and was not significantly different between day and night. The current showed no inactivation during the 200 ms test pulse when measured as a ratio of current amplitude at the beginning (50ms) and the end of the pulse (20mV: 1.07 ± 0.03;

30 mV: 1.01 ± 0.03; 40mV: 0.99 ± 0.03 and 50mV: 0.93 ± 0.02; n = 17). Deactivation of sDR currents occurred with a time constant of 3.94 ± 0.35 ms (n = 10) and did not vary from day to night (Day: 4.31 ± 0.62 ms, n = 5; Night: 3.58 ± 0.32 ms, n = 5).

The fDR currents were also detected in every SCN neuron (n = 74), although the amplitude varied by phase. The fDR currents were isolated by subtraction ($I_{control} - I_{4\text{-}AP}$, Fig. 2a) using the pulse protocol described above[21,22]. We found that 4–AP (0.5mM) does not significantly attenuate the transient A–type K^+ current (8 ± 2% reduction, n = 8). The fDR current in dSCN neurons showed an activation curve with a midpoint potential of 6.8 ± 0.4 mV and steep activation characteristics (slope factor k = 8.9 ± 0.4 mV, n = 9, Fig. 2b) during the day. The activation kinetics were similar during the night (midpoint 7.1 ± 0.7 mV, slope factor k = 11.6 ± 0.7 mV, n = 7, Fig. 2b). The 20–80% rise time was voltage–dependent in dSCN neurons (ranging from 18.4 ms at 0 mV to 1.6 ms at 50 mV, n = 16, Fig. 2c) and was not significantly different between day and night. The current showed no inactivation during the 200 ms test pulse as characterized by the ratio of current amplitude at the beginning (50 ms) and the end of the pulse (20 mV: 1.12 ± 0.12; 30 mV: 0.98 ± 0.03; 40 mV: 1.01 ± 0.05 and 50 mV: 1.01 ± 0.04; n = 23). Deactivation of fDR currents occurred with a time constant of 2.47 ± 0.14 ms (n = 16) and did not vary from day to night (Day: 2.51 ± 0.18 ms, n = 7; Night: 2.38 ± 0.22 ms, n = 9). TEA (1 mM) was also used to isolate and measure fDR currents in the dSCN during the day and night. There were no differences in the kinetics and magnitude of the currents isolated with 4-AP (0.5 mM) or TEA (1 mM).

Circadian variation in fDR currents

The fDR current traces generated by subtraction ($I_{control} - I_{4\text{-}AP}$, Fig. 2a) were used to determine the current-voltage relation in the dSCN during day, early night and late night. The magnitude of the fDR currents was significantly greater during the day (n = 15; $P < 0.05$) compared to early night (n = 10, Fig. 3a) and late night (n = 7, data not shown). The sDR current traces generated by subtraction ($I_{1\ mM\ TEA} - I_{20\ mM\ TEA}$, Fig. 1b) were used to determine the current-voltage relation in the dSCN during day and night. There was no significant difference in the magnitude of sDR currents during the day (n = 11) compared to the night (n = 9, Fig. 3b). To determine if the observed rhythm in fDR currents between day and night was circadian, we performed similar experiments on dSCN neurons from animals housed in constant darkness (Fig. 3c). We found the same relationship in the magnitude of fDR currents in the dSCN between subjective day (n = 6, $P < 0.02$) and subjective night (n = 6), confirming that the rhythm is sustained in constant darkness and is endogenously generated. In contrast, there was no significant rhythm in sDR currents between subjective day (n = 6) and subjective night (n = 6, Fig. 3d).

Kv3.1b and Kv3.2 are expressed throughout the SCN

The Kv3.1 and Kv3.2 channels are responsible for the fDR currents[15]. In order to examine the pattern of expression of these channels in the SCN, antibodies raised against Kv3.1b and Kv3.2 channels were utilized (Fig. 4). Mice were perfused at day (zeitgeber time 4–6) and night (zeitgeber time 14–16). Tissue sections from each time point were grouped and immunohistochemical procedures were run in parallel to avoid procedural artifacts and to ensure consistency. The Kv3.1b immunoreactivity was evident throughout the SCN and most cell bodies were labeled. Staining was robust in both the dorsal and ventral regions of the SCN. This general pattern was seen throughout the rostral to caudal extent of the SCN. The mean number of immuno-positive neurons per SCN section was significantly higher during the day than during the night (Day: 1941 ± 11 cells, n = 5 vs. Night: 59 ± 24 cells, n = 5; $P < 0.001$). Optical analysis of digital images of these sections indicated that the immuno-positive neurons during the day were significantly darker than the neurons during the night (Day: 0.42 ± 0.01 OD vs. Night: 0.27 ± 0.01 OD; $P < 0.001$). An antibody raised against Kv3.2 also labeled cell

bodies throughout the dorsal and ventral SCN. The staining was most robust in the rostral and central SCN regions with relatively less staining present in the caudal aspects of the nucleus. The mean number of immuno-positive neurons per SCN section was also significantly higher during the day (Day: 103 ± 13 cells, $n = 6$ vs. Night: 40 ± 19 cells, $n = 5$; $P < 0.02$). Again optical density measurements indicated that the immuno-positive neurons were significantly darker in the day (Day: 0.37 ± 0.01 OD vs. Night: 0.25 ± 0.01 OD; $P < 0.001$). These day/night differences were not seen in the number (Day: 80 ± 9 cells vs. Night: 73 ± 7 cells) or optical density (Day: 0.46 ± 0.02 OD vs. Night: 0.43 ± 0.01 OD) of immunoreactive cells in the piriform cortex region of the same sections. Overall, the immunocytochemistry analysis indicates that Kv3.1b and Kv3.2 channels are expressed within broad regions of the SCN and expression of these channels is significantly higher in the day.

Regulation of spontaneous firing rate by fDR currents

Finally, we determined the contribution of fDR currents to the spontaneous firing rate (SFR) in SCN neurons with two sets of experiments. Using the current-clamp recording technique in the perforated–patch configuration, we applied either 0.5 mM 4-AP or 1 mM TEA to dSCN neurons and found that blocking fDR currents reduced SFR by 41 ± 4 % (5.32 to 3.13 Hz, $n = 14$, $P < 0.001$, Fig. 5a) during the day in the presence of bicuculline (25 μM) and cadmium (100 μM). This treatment prolonged repolarization and reduced the amplitude and duration of the after hyperpolarization (AHP) of the action potential in nearly every cell treated (11/14, Fig. 5b). The reduction in SFR was long–lasting and not relieved by up to 30 min of washout ($n = 5$). Three of the fourteen dSCN neurons recorded during the day did not respond to treatment.

Application of 0.5 mM 4-AP or 1 mM TEA reduced SFR of dSCN neurons during the early night by 20 ± 5 % (2.80 to 2.08 Hz, $n = 13$, Fig. 5c). These treatments significantly lengthened repolarization and reduced the amplitude and duration of the AHP in nearly every cell treated (7/11, Fig. 5d). Three of the eleven dSCN neurons recorded during the early night did not respond significantly to treatment with either 4-AP or TEA. During the late night, treatment of dSCN neurons with 0.5 mM 4-AP or 1 mM TEA reduced SFR by 9 ± 2 % (2.25 to 2.08 Hz, $n = 7$, data not shown). Treatment resulted in changes to the action potential waveform that were identical to those observed during early night in nearly every cell treated (5/7, Fig. 5e-f). One of the seven dSCN neurons recorded during the late night did not respond significantly to treatment. Overall, a comparison of all current clamp recordings from dSCN showed significantly higher SFR during the day (5.32 Hz) compared to early night (2.80 Hz, $P < 0.001$) and late night (2.25 Hz, $P < 0.002$, Fig. 6a). After application of 0.5 mM 4-AP to eliminate the fDR current, the SFR was not significantly different between any time points ($P > 0.5$, Fig. 6a), suggesting that the activation of the fDR was necessary for the daily modulation of neuronal activity in dSCN. Blocking the fDR current during the day resulted in a much greater reduction in SFR (41 %) compared to early night (23 %) and late night (9 %, Fig. 6b).

It is possible that blocking these K^+ channels may have different impact on the acute firing rate of SCN neurons than on the longer-term circadian rhythm of the electrical activity. Therefore, in the final set of experiments, circadian rhythms of multi-unit activity were recorded from mouse brain slice preparations with stationary electrodes. Data from control tissue (Fig. 7a-b) all showed high activity during the middle of the projected light phase (mid–subjective day) and low activity during the projected dark phase (mid-subjective night). In contrast, this rhythm was greatly reduced or eliminated in those slices treated with 0.5 mM 4-AP (Fig. 7c-d). In order to quantify this loss of rhythmicity, the slopes of the activity rhythm measured between zeitgeber time 23 and 4 were analyzed. The average slope of the control recordings was 34 ± 6 Hz/h ($n = 6$) whereas the 4–AP treated slices exhibited a slope of 1.5 ± 3 Hz/h ($n = 6$). The control, but not the 4–AP treated slope was significantly different from

zero ($P < 0.01$). Moreover, no significant positive slope was detected in 4–AP treated slices during the whole recording as tested in six intervals (3 h) between zeitgeber time 15.5 and 9.5. At the end of the experiment, all of the slices exhibited a robust increase in firing in response to NMDA (5 μM, data not shown) indicating viability of the slice at the tissue level.

Discussion

In the present study, perforated and whole–cell patch electrophysiological techniques were utilized to record outward K^+ currents in SCN neurons. We provide the first description of a circadian modulation of a fDR K^+ current in SCN neurons. Two different pharmacological treatments (4-AP and TEA) were used to isolate sDR and fDR currents[21,22]. As described in other neurons, these currents activate only at depolarized membrane potentials and have rapid activation and deactivation kinetics. In the SCN, the fDR current begins to activate at −20 mV and most neurons exhibit half-activation voltages around 6 mV. Once activated, the fast kinetics of this current allow neurons to quickly repolarize after generation of action potentials without altering the spike threshold or action potential height[15]. Previous studies have found these currents in cell populations with high firing rates in sensory[20] and motor circuits[16]. The presence of this current should allow SCN neurons to discharge at higher rates during the day without adaptation. The fDR current is sensitive to both 4-AP (0.5 mM) and TEA (1 mM), giving us pharmacological tools to investigate the contribution of this current to the frequency of action potential generation in the SCN. Using perforated patch recording techniques to minimize cell dialysis and obtain reliable SFR recordings[23], we found that acutely blocking the fDR with 0.5 mM 4-AP or 1 mM TEA significantly decreases the firing rate of SCN neurons during the day so that the day/night difference in SFR was eliminated. This is an unusual feature of the fDR because the blockade of most K^+ currents would be expected to increase firing rate. Finally, using extracellular recordings of rhythms in multi–unit activity, we found that longer-term application of 4-AP (0.5 mM) prevented expression of diurnal rhythms in electrical activity recorded from SCN tissue.

Based on our observations, we believe that the fDR K^+ current is necessary for the expression of the circadian rhythm in the frequency of action potentials. We found that the rhythm in the magnitude of this current is correlated with the rhythm in electrical discharge in that both peak during the day and are low during the night. This rhythm in amplitude continues in constant darkness and appears to be a circadian rhythm expressed at the level of individual SCN neurons. Other properties of the current such as voltage-dependence and activation/deactivation kinetics did not change with the daily cycle. The sDR current did not show a diurnal or circadian rhythm in amplitude or kinetic parameters in the dSCN. In addition, when the fDR was acutely blocked with 4-AP, the frequency of firing in the SCN was significantly reduced with the largest effects in dSCN neurons recorded during the day. Longer treatments of 4-AP prevented the daily rhythm of firing in the SCN. Although the evidence presented points to a crucial role of the fDR in diurnal and circadian SFR modulation, this current can not be responsible for the initial membrane depolarization at dawn. The fDR only acts in a range of voltages that are depolarized relative to resting membrane potential of SCN neurons. Another class of current must be responsible for driving action potential generation in order to activate fDR channels.

SCN neurons are known to exhibit a slowly inactivating sodium current, which activates around −65mV[24,25]. While it is not known if this current exhibits a circadian rhythm, blocking this sodium current inhibits spontaneous firing[25]. In addition, previous work found evidence for a daily rhythm in a L-type calcium current[26]. These sodium and calcium currents likely play a critical role in moving the SCN neuron into a voltage-range in which the fDR would be activated. Finally, electrophysiological measurements from SCN neurons suggest that input resistance also peaks during the day[23,27,28]. These observations suggest, when SCN neurons are at their resting membrane potential, the net current flow through ion channels is lower

during the day. Since the membrane is also depolarized during the day[23], the closed channels are likely to be K^+ channels. Important support for this model comes from the observation that a TEA-sensitive K^+ current is critical for the daily change in input resistance[28]. The identity of these channels are not yet known and these studies raise the possibility that a whole set of currents change rhythmically in the SCN as the cell moves from a "inactive/down" state during the night to an "active/up" state during the day. However, not all currents within the SCN are rhythmically regulated and the sDR (present study), a barium-sensitive K^+ current[10] and H-currents[29] all appear to be constant from day to night.

The mechanisms underlying the daily rhythm in fDR currents is not known. Our immunocytochemical evidence clearly indicates the presence of the Kv3.1b and Kv3.2 channels in the SCN and suggests that expression of these channel proteins is rhythmically regulated. It is possible that the *KCNC1* (also known as Kv3.1) and *KCNC2* (Kv3.2) genes are rhythmically regulated as many genes in this region exhibit transcriptional rhythms[30] and the promotor region of the *KCNC1* gene contains both CRE and AP-1 sites[31]. Previous studies have found evidence that calcium, cyclic nucleotides, and immediate early genes are rhythmic in the SCN and we might expect to see a rhythm in the expression of the genes coding for the fDR. In *Drosophila*, circadian rhythms in mRNA coding for a regulatory protein associated with Ca^{2+}-sensitive K^+ channels have been described[32,33]. Furthermore, in mammalian cardiac tissue, diurnal variation in the expression of genes coding for two K^+ channels (Kv1.5 and Kv4.2) has been described[34]. However, the regulation need not be transcriptional and post-translational modifications could also be responsible for the daily rhythms. Outside of the SCN, numerous studies have demonstrated the importance of kinase/phosphotase activity in mediating short-term changes in channel function that alter electrical excitability[8]. In chick photoreceptors, circadian oscillations in chick cone cGMP-gated channels have been well described[35]. Within the SCN, circadian patterns of phosphorylation appear to be critical for the basic molecular feedback loop driving circadian rhythms with the involvement of casein kinases appears to be particularly important[36]. Regardless of the underlying mechanism, the work described in the present study identifies a specific K^+ current that is under the regulatory control of the molecular circadian feedback loop and demonstrates that this current is necessary for the daily rhythm in frequency of action potential generation that lies at the heart of the SCN oscillator.

Methods

In all studies, the recommendations for animal use and welfare, as dictated by the UCLA Division of Laboratory Animals and the guidelines from the National Institutes of Health, or the Animal Experiments Ethical Committee of the Leiden University Medical Center, were followed.

Behavioral Measurements

Male mice, at least 21 days of age, were housed individually and their wheel–running activity recorded (Mini Mitter Co. Bend, OR). Zeitgeber time is used to describe the projected time based on the previous light cycle, with lights–on defined as ZT 0. Circadian time is used when mice were in constant darkness and the onset of activity defined as circadian time 12. When necessary, mice were sacrificed in darkness using an infrared viewer. In all cases, mice were sacrificed 1 h before recording.

Whole Cell Patch Clamp Electrophysiology

Brain slices were prepared using standard techniques from mice (C57/Bl6) between 30–50 days of age. Methods including solutions were identical to those described previously[17]. For perforated patch recordings, standard internal was used to fill the tip of the patch pipette.

Amphotericin was dissolved in DMSO and mixed with standard internal at 0.2 mM for backfilling the patch pipette. Recordings were obtained with an Axon Instruments 200B amplifier and monitored on-line with pCLAMP (Axon Instruments, Foster City, CA). To minimize changes in offset potentials with changing ionic conditions, the ground path used a KCl agar bridge. Whole cell capacitance and electrode resistance were neutralized and compensated (50–80%). Series and input resistance was monitored repeatedly by checking the response to small pulses in a passive potential range. Series resistance was not compensated and the maximal voltage error due to this resistance was calculated to be 6 mV. The access resistance of these cells ranged from 15–35 MΩ in the whole cell voltage-clamp configuration while the cell capacitance was typically between 6–18 pF.

Current traces were recorded with pClamp using the whole cell voltage-clamp recording configuration, then analyzed using ClampFit. Delayed rectifier K^+ currents were isolated pharmacologically using a voltage-step protocol in the whole cell voltage-clamp configuration. The protocol consisted of a 100 ms prepulse at −90 mV followed by a 250 ms step at progressively depolarized potentials. Leak subtraction was performed during acquisition using a p/4 protocol, which utilizes four sub-pulses with ¼ of the test pulse amplitude and reversed polarity given from a holding potential of −70 mV. Current traces from treatment were subtracted from control to isolate delayed rectifier currents. Both 4-AP (0.5 mM) and TEA (1 mM) were used to isolate fDR currents, whereas high-concentration TEA (20 mM) was used to isolate sDR currents. Current measurements were performed in control solution and after 5–7 min of drug treatment in each cell. Activation curves were generated using data collected from the voltage step protocol outlined above and fit with a Boltzman function $f(Vm) = 1/(1+\exp(-(Vm-Vhalf)/k))$, where *Vm* is the membrane potential, *Vhalf* is the membrane potential at 0.5 and *k* is the slope factor. Inactivation curves were generated by using the following protocol in the whole cell voltage clamp configuration: 100 ms prepulses of varying potentials (−100 mV to −30 mV, 5 mV steps) followed by a 900 ms step at +50 mV to elicit maximal current. Data was fit with the Boltzman function described for activation curves and 20–80% rise time measurements were made on current traces. SFR and action potential waveforms were recorded with pClamp using current–clamp in the whole cell perforated patch configuration. No current was injected during recording. After a baseline SFR was established, drug treatment began within 5 min of obtaining the perforate patch configuration (access resistance less than 100 MΩ).

Extracellular Recording

The multiunit activity rhythms of SCN neurons were measured as described[37]. Coronal slices (500 μm) were prepared from male C57 Bl/6 mice at the beginning of the subjective day. The slices were kept submerged with a thin fork in a laminar flow chamber (35.5°C). The slices contained at least 50% of the rostro-caudal extent of the SCN, and all of the ventro-dorsal extent. Extracellular electrical activity of SCN neurons was measured by platinum/iridium electrodes, subsequently amplified and bandwidth-filtered[38]. Action potentials with signal-to-noise ratio of 2:1 (noise < 5 μV from baseline) were selected by spike triggers and counted electronically every 10 s for about one circadian cycle. The positions of the electrodes and spike trigger settings were not changed during the experiment. Linear fits were performed on the multi–unit activity data between zeitgeber time 23 and 4 and the slopes of the resulting lines were determined. A significant positive slope at this circadian time is indicative of a typical rhythm in electrical activity. The obtained slopes from control and experimental slices were tested against zero using a one-sided t-test ($P < 0.05$). The individual examples in the figures were smoothed with a box filter for clearer presentation of the data.

Immunocytochemistry

The methods were similar to those previously described[39]. Polyclonal antibodies for Kv3.1b and Kv3.2 raised in rabbit were purchased (Alomone Labs, Jerusalem, Israel). A dilution series was performed for both antibodies with optimal dilution found to be 1:150 for the Kv3.2 and 1:400 for the Kv3.1b. The anti-Kv3.1b was raised to amino acids 567–585 which is a sequence unique to the Kv3.1b splice variant, while anti-Kv3.2 recognizes a sequence common to all known splice variants of Kv3.2, amino acids 184–204. Tissue sections from each time point were grouped and processed in parallel to avoid procedural artifacts and to ensure consistency. Immunocytochemical controls included the omission of primary and secondary antisera and preabsorption of antibodies with appropriate peptide epitopes. We found that that the omission of primary antibodies and preabsorption with appropriate epitopes blocked all staining.

For each mouse, images were taken from one section from each of three regions (rostral, middle, and caudal) using a SPOT camera system (Diagnostic Instruments, Sterling Heights, Michigan). All immuno-positive cells within the SCN of these three sections were counted manually at 400X with the aid of a grid. All immuno-positive cells within the grid were counted equally without regard to the intensity of the staining. Counts were done by 2 observers blind to treatment protocol and the results averaged. In order to have some measure of the intensity of staining, optical density measurements were also undertaken using SigmaScan Pro software (SPSS, Chicago, IL, USA). For this analysis, digital images were converted to a 8-bit grey scale in which each pixel would register a grey level (GL) value between 0 (dark) and 255 (white). SCN neurons were manually outlined so that the program could determine the average GL per neuron. The optical density was then calculated as OD = −log (GL neuron/GL max). The microscope, lighting, and software parameters were held constant to allow comparisons to be made in the OD measurements between tissue sections. Cell counts and optical density measurements were also made in the piriform cortical region of the same sections containing the SCN.

Statistical analyses

Between group differences were first evaluated using an analysis of variance (ANOVA) to determine if there were any significant differences among means of all groups. Post hoc pairwise comparisons were then performed using t–tests or Mann-Whitney rank sum tests when appropriate. Values were considered significant if $P < 0.05$. All tests were performed using SigmaStat (SPSS, Chicago, IL, USA). In the text, values are shown as mean ± SEM.

Acknowledgements

Supported by National Institute of Health HL64582, NS043169, and MH68087. We would like to thank H. Duindam for excellent technical assistance. We would also like to thank E. Herzog and N. Wayne for comments on a draft of the manuscript.

References

1. van Esseveldt KE, Lehman MN, Boer GJ. The suprachiasmatic nucleus and the circadian timekeeping system revisited. Brain Res Rev 2000;33:34–77. [PubMed: 10967353]
2. Gillette MU. Cellular and biochemical mechanisms underlying circadian rhythms in vertebrates. Curr Opin Neurobiol 1997;7:797–804. [PubMed: 9464980]
3. King DP, Takahashi JS. Molecular genetics of circadian rhythms in mammals. Annu Rev Neurosci 2000;23:713–742. [PubMed: 10845079]
4. Reppert SM, Weaver DR. Molecular analysis of mammalian circadian rhythms. Annu Rev Physiol 2001;63:647–676. [PubMed: 11181971]
5. Nitabach MN, Blau J, Holmes TC. Electrical silencing of Drosophila pacemaker neurons stops the free–running circadian clock. Cell 2002;109:485–495. [PubMed: 12086605]

6. Harmar AJ, et al. The VPAC2 Receptor is essential for circadian function in the mouse suprachiasmatic nuclei. Cell 2002;109:497–508. [PubMed: 12086606]
7. Schaap J, Pennartz CM, Meijer JH. Electrophysiology of the circadian pacemaker in mammals. Chronobiol Int 2003;20:171–188. [PubMed: 12723879]
8. Hille, B. *Ion Channels of Excitable Membranes* Sinauer Associates, Sunderland, MA, USA, 2001
9. Bouskila Y, Dudek FE. A rapidly activating type of outward rectifier K^+ current and A–current in rat suprachiasmatic nucleus neurones. J Physiol 1995;488:339–350. [PubMed: 8568674]
10. De Jeu M, Geurtsen A, Pennartz CM. A Ba^{2+}–sensitive K^+ current contributes to the resting membrane potential of neurons in rat suprachiasmatic nucleus. J Neurophysiol 2002;88:869–878. [PubMed: 12163538]
11. Cloues RK, Sather WA. Afterhyperpolarization regulates firing rate in neurons of the suprachiasmatic nucleus. J Neurosci 2003;23:593–604.
12. Teshima K, Kim SH, Allen CN. Characterization of an apamin–sensitive potassium current in suprachiasmatic nucleus neurons. Neuroscience 2003;120:65–73. [PubMed: 12849741]
13. Michel S, Geusz ME, Zaritsky JJ, Block GD. Circadian rhythm in membrane conductance expressed in isolated neurons. Science 1993;259:239–241. [PubMed: 8421785]
14. Michel S, Manivannan K, Zaritsky JJ, Block GD. A delayed rectifier current is modulated by the circadian pacemaker in Bulla. J Biol Rhythms 1999;14:141–150. [PubMed: 10194651]
15. Rudy B, McBain CJ. Kv3 channels: voltage–gated K^+ channels designed for high–frequency repetitive firing. Trends Neurosci 2001;24:517–526. [PubMed: 11506885]
16. Baranauskas G, Tkatch T, Nagata K, Yeh JZ, Surmeier DJ. Kv3.4 subunits enhance the repolarizing efficiency of Kv3.1 channels in fast–spiking neurons. Nat Neurosci 2003;6:258–266. [PubMed: 12592408]
17. Itri J, Colwell CS. Regulation of inhibitory synaptic transmission by vasoactive intestinal peptide (VIP) in the mouse suprachiasmatic nucleus. J Neurophysiol 2003;90:1589–1597. [PubMed: 12966176]
18. Hamada T, Antle MC, Silver R. Temporal and spatial expression patterns of canonical clock genes and clock–controlled genes in the suprachiasmatic nucleus. Eur. J. Neurosci 2004;19:1741–1748. [PubMed: 15078548]
19. Yamaguchi S, et al. Synchronization of cellular clocks in the suprachiasmatic nucleus. Science 2003;302:1408–1412. [PubMed: 14631044]
20. Wang LY, Gan L, Forsythe ID, Kaczmarek LK. Contribution of the Kv3.1 potassium channel to high–frequency firing in mouse auditory neurones. J Physiol 1998;509:183–194. [PubMed: 9547392]
21. Martina M, Schultz JH, Ehmke H, Monyer H, Jonas P. Functional and molecular differences between voltage–gated K^+ channels of fast–spiking interneurons and pyramidal neurons of rat hippocampus. J Neurosci 1998;18:8111–8125. [PubMed: 9763458]
22. Kirsch GE, Drewe JA. Gating–dependent mechanism of 4–aminopyridine block in two related potassium channels. J Gen Physiol 1993;102:797–816. [PubMed: 8301258]
23. Schaap J, et al. Neurons of the rat suprachiasmatic nucleus show a circadian rhythm in membrane properties that is lost during prolonged whole–cell recording. Brain Res 1999;815:154–166. [PubMed: 9974136]
24. Pennartz CM, Bierlaagh MA, Geurtsen AM. Cellular mechanisms underlying spontaneous firing in rat suprachiasmatic nucleus: involvement of a slowly inactivating component of sodium current. J Neurophysiol 1997;78:1811–1825. [PubMed: 9325350]
25. Kononenko NI, Shao LR, Dudek FE. Riluzole–sensitive slowly inactivating sodium current in rat suprachiasmatic nucleus neurons. J Neurophysiol 2004;91:710–718. [PubMed: 14573554]
26. Pennartz CM, de Jeu MT, Bos NP, Schaap J, Geurtsen AM. Diurnal modulation of pacemaker potentials and calcium current in the mammalian circadian clock. Nature 2002;416:286–290. [PubMed: 11875398]
27. Jiang ZG, Yang Y, Liu ZP, Allen CN. Membrane properties and synaptic inputs of suprachiasmatic nucleus neurons in rat brain slices. J Physiol 1997;499:141–159. [PubMed: 9061646]

28. Kuhlman SJ, McMahon DG. Rhythmic regulation of membrane potential and potassium current persists in SCN neurons in the absence of environmental input. Eur J Neurosci 2004;20:1113–1117. [PubMed: 15305881]
29. de Jeu MT, Pennartz CM. Functional characterization of the H–current in SCN neurons in subjective day and night: a whole–cell patch–clamp study in acutely prepared brain slices. Brain Res 1997;767:72–80. [PubMed: 9365017]
30. Panda S, et al. Coordinated transcription of key pathways in the mouse by the circadian clock. Cell 2002;109:307–320. [PubMed: 12015981]
31. Gan L, Kaczmarek LK. When, where, and how much? Expression of the Kv3.1 potassium channel in high–frequency firing neurons. J Neurobiol 1998;37:69–79. [PubMed: 9777733]
32. McDonald MJ, Rosbash M. Microarray analysis and organization of circadian gene expression in *Drosophila*. Cell 2001;107:567–578. [PubMed: 11733057]
33. Ceriani MF, et al. Genome–wide expression analysis in *Drosophila* reveals genes controlling circadian behavior. J Neurosci 2002;22:9305–9319. [PubMed: 12417656]
34. Yamashita T, et al. Circadian variation of cardiac K^+ channel gene expression. Circulation 2003;107:1917–1922. [PubMed: 12668525]
35. Ko GY, Ko ML, Dryer SE. Circadian regulation of cGMP–gated channels of vertebrate cone photoreceptors: role of cAMP and Ras. J Neurosci 2004;24:1296–304. [PubMed: 14960600]
36. Reppert SM, Weaver DR. Coordination of circadian timing in mammals. Nature 2002;418:935–941. [PubMed: 12198538]
37. Meijer JH, Schaap J, Watanabe K, Albus H. Multiunit activity recordings in the suprachiasmatic nuclei: in vivo versus in vitro models. Brain Res 1997;753:322–327. [PubMed: 9125419]
38. Schaap J, Albus H, vanderLeest HT, Eilers PH, Detari L, Meijer J. H Heterogeneity of rhythmic suprachiasmatic nucleus neurons: Implications for circadian waveform and photoperiodic encoding. Proc Nat Acad Sci 2003;100:15994–999. [PubMed: 14671328]
39. Michel S, Itri J, Colwell CS. Excitatory Mechanisms in the Suprachiasmatic Nucleus: the role of AMPA/KA glutamate receptors. J Neurophysiol 2002;88:817–828. [PubMed: 12163533]

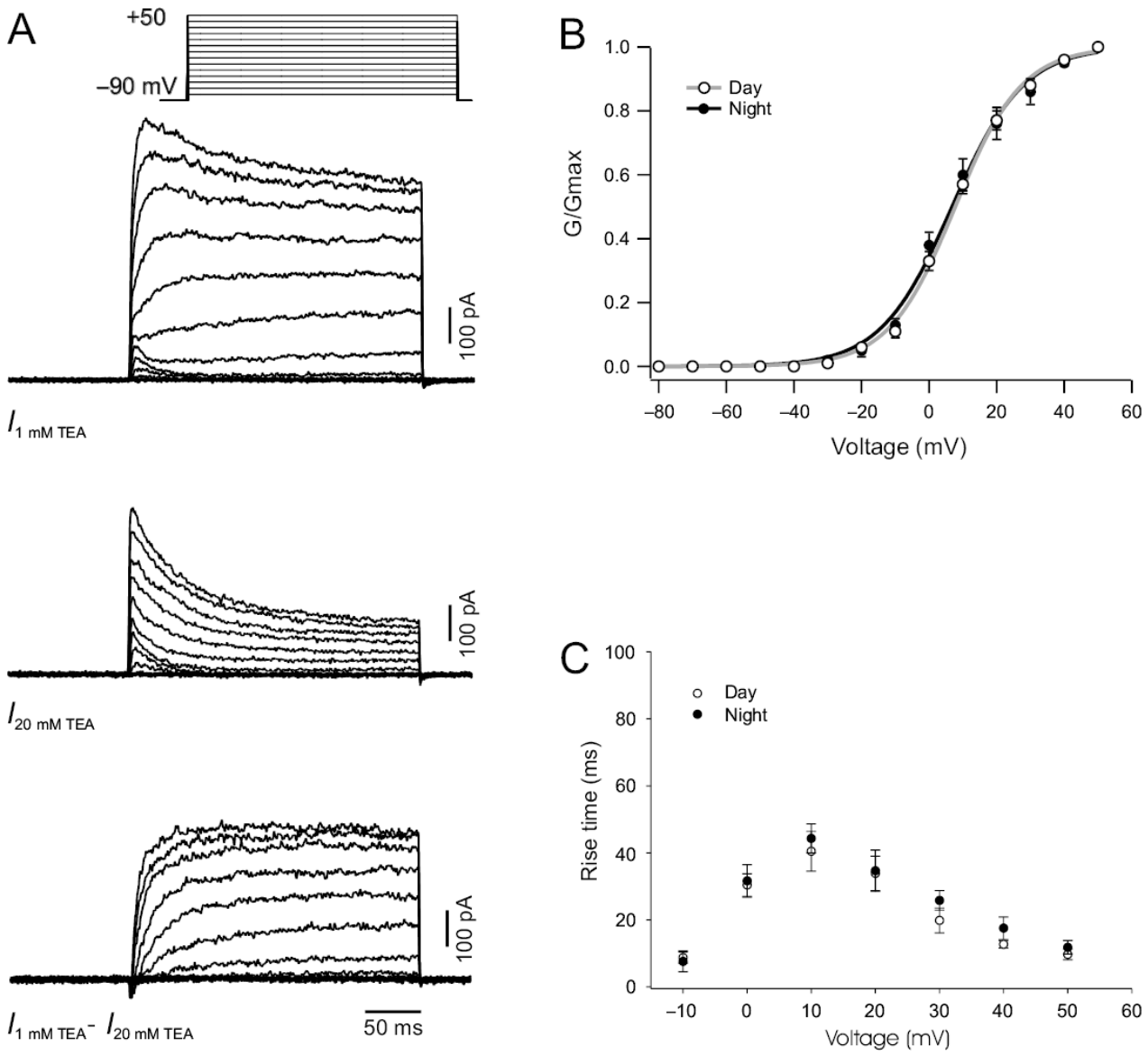

Fig. 1.

Characterization of sDR K^+ currents in SCN neurons. (**a**) $I_{1\ mM\ TEA}$ current traces were generated by using the voltage step protocol with a prepulse potential of −90 mV and test pulse potentials ranging from −80 to +50 mV (10 mV increments). $I_{20\ mM\ TEA}$ current traces were generated using the same protocol after 5 min treatment with 20 mM TEA. Bottom trace shows example of a sDR current trace isolated by subtracting $I_{20\ mM\ TEA}$ from $I_{1\ mM\ TEA}$. (**b**) Activation curves generated in dSCN neurons during the day and night by applying a hyperpolarizing prepulse (100 ms at −90 mV) followed by 900 ms voltage pulses at progressively depolarized potentials (−80 to +40 mV, 10 mV steps). **(c)** The curves show the 20–80% rise time measurements for sDR currents recorded during the day and night.

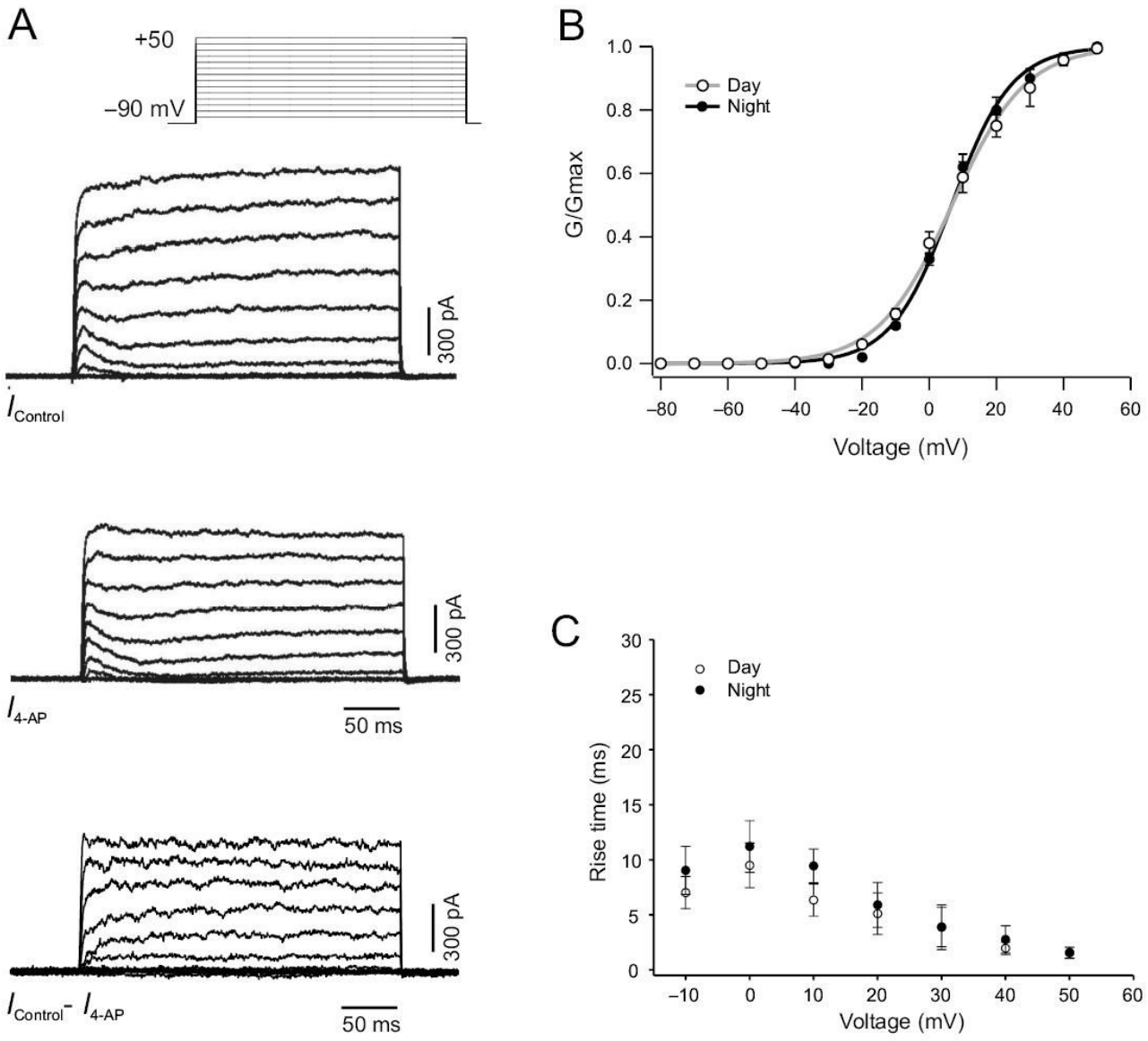

Fig. 2.

Characterization of fDR K^+ currents in SCN neurons. (**a**) $I_{control}$ current traces were generated by using the voltage step protocol with a prepulse potential of −90 mV and test pulse potentials ranging from −80 to +50 mV (10 mV increments, *bottom*). $I_{4\text{-}AP}$ current traces were generated using the same protocol after 5 min treatment with 0.5 mM 4-AP. Bottom trace shows example of a fDR current trace isolated by subtracting $I_{4\text{-}AP}$ from $I_{control}$. (**b**) Activation curves generated in dSCN neurons during the day and night by applying a hyperpolarizing prepulse (100 ms at −90 mV) followed by 900 ms voltage pulses at progressively depolarized potentials (−80 to +40 mV, 10 mV steps). (**c**) 20–80% rise time measurements for fDR currents recorded during the day and night.

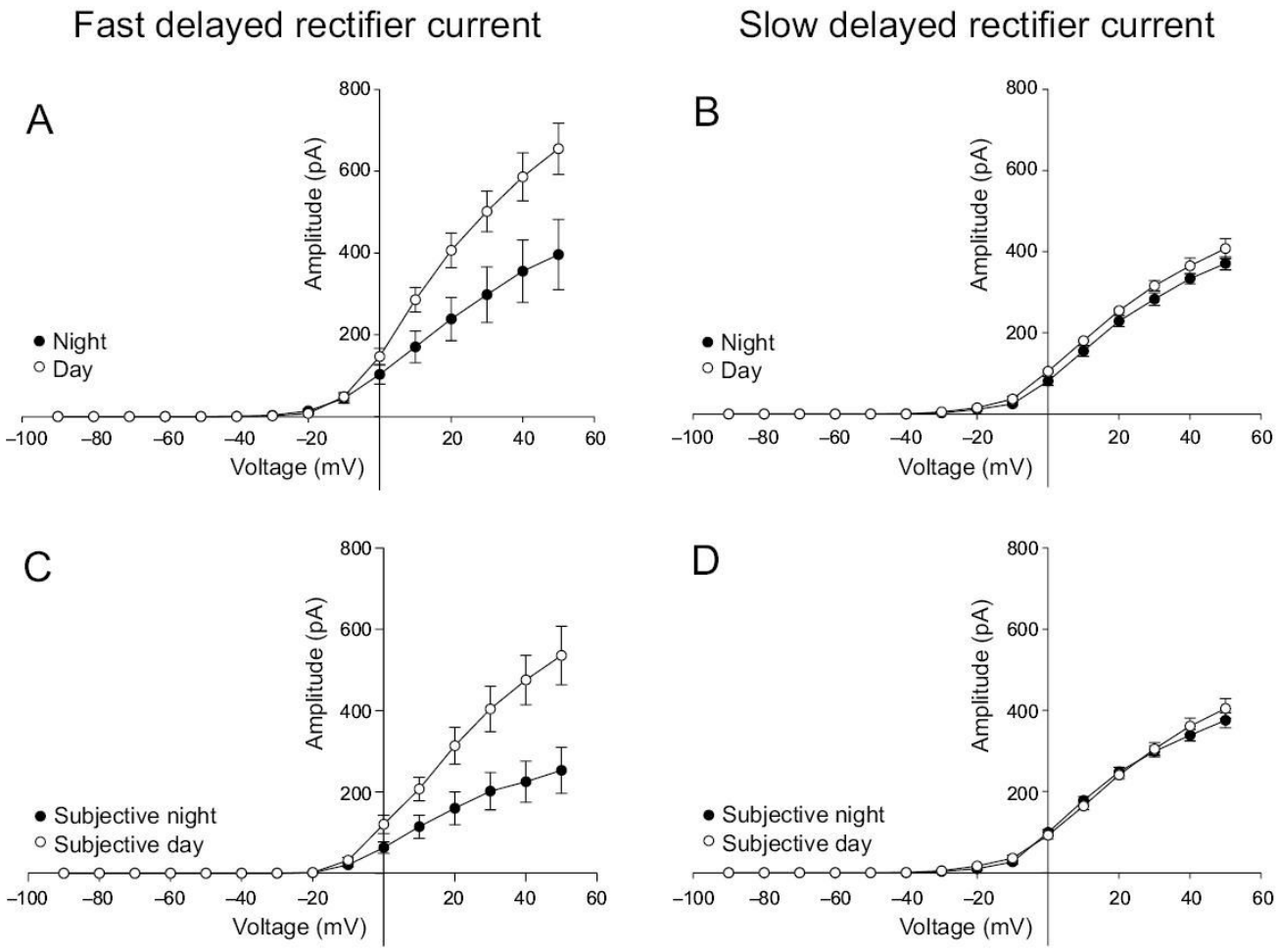

Fig 3.

Current-voltage relationship of delayed rectifier K^+ currents in the mouse dSCN. (**a**) The fDR currents recorded during the day were significantly greater than those recorded during the night. (**b**) In contrast, the sDR currents did not vary between day and night. (**c**) The fDR currents recorded in the subjective day were significantly greater compared to subjective night. (**d**) The sDR currents did not vary between subjective day and night.

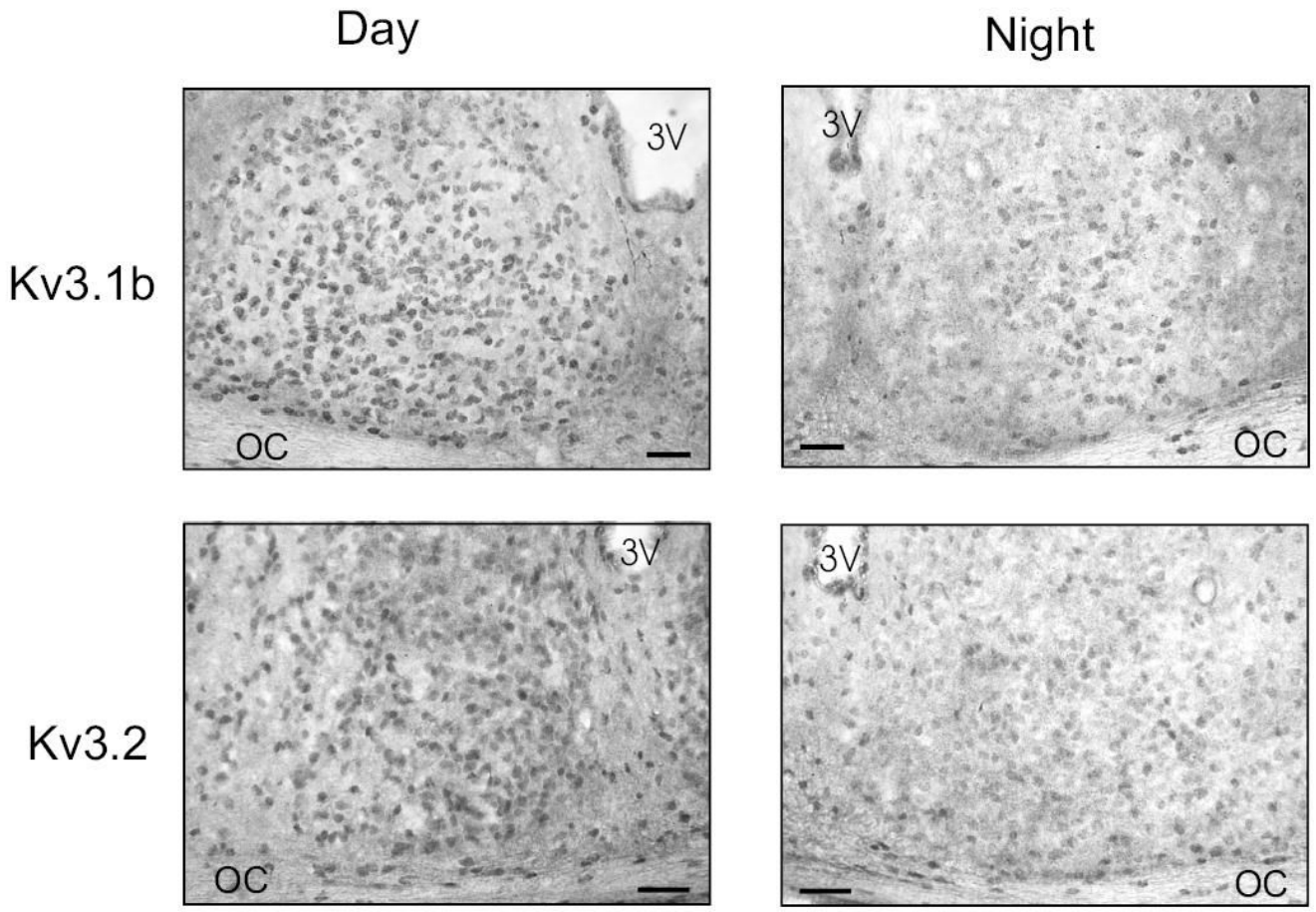

Fig. 4.

Photomicrographs showing immunoreactivity for Kv3.1b and Kv3.2 in the SCN during the day and night. 3V, third ventricle; OC, optic chiasm. Top panels: The Kv3.1b immunoreactivity was robust throughout the SCN including the ventral lateral portions as well as a dorsal region of SCN near the 3rd ventricle. Positive staining was seen throughout the rostral to caudal extent of the SCN. The number of immuno-positive cells as well as the density of the staining were significantly higher in the day than in the night. Bottom panels: Kv3.2 immunoreactivity was also seen on cell bodies throughout the SCN. The staining was most robust in the rostral and central aspects of the SCN. Tissue collected from adult C57 BL/6 mice that were perfused during the day or night. Scale bar = 50 μm.

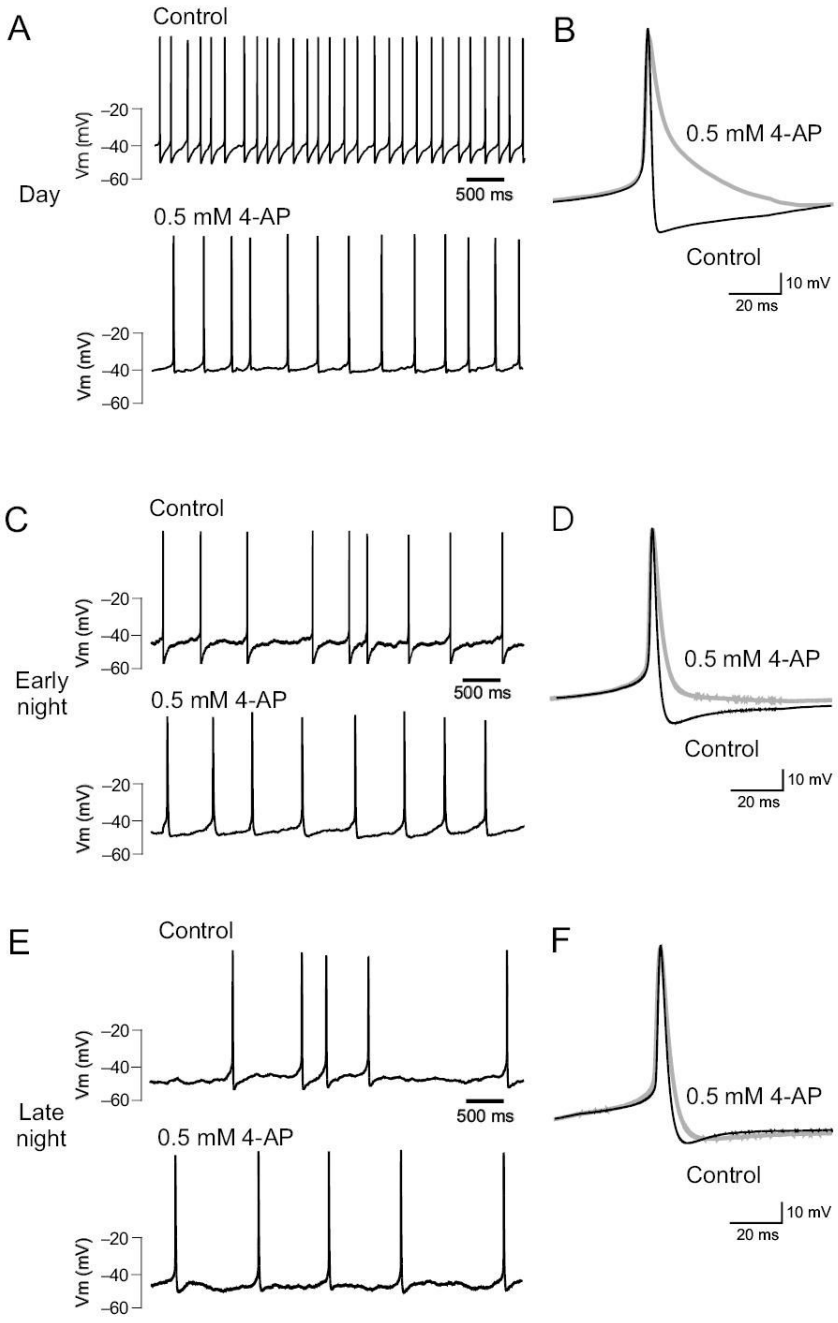

Fig. 5.

Blocking fDR currents significantly reduces the firing rate of SCN neurons. Bath-application of 0.5 mM 4-AP significantly reduced electrical activity in dSCN neurons recorded during the day (**a**), early night (**c**), and late night (**e**). Analysis of the average action potential waveform (**b, d, f**) shows that reduction of fDR currents prolongs repolarization and reduces the magnitude of AHP.

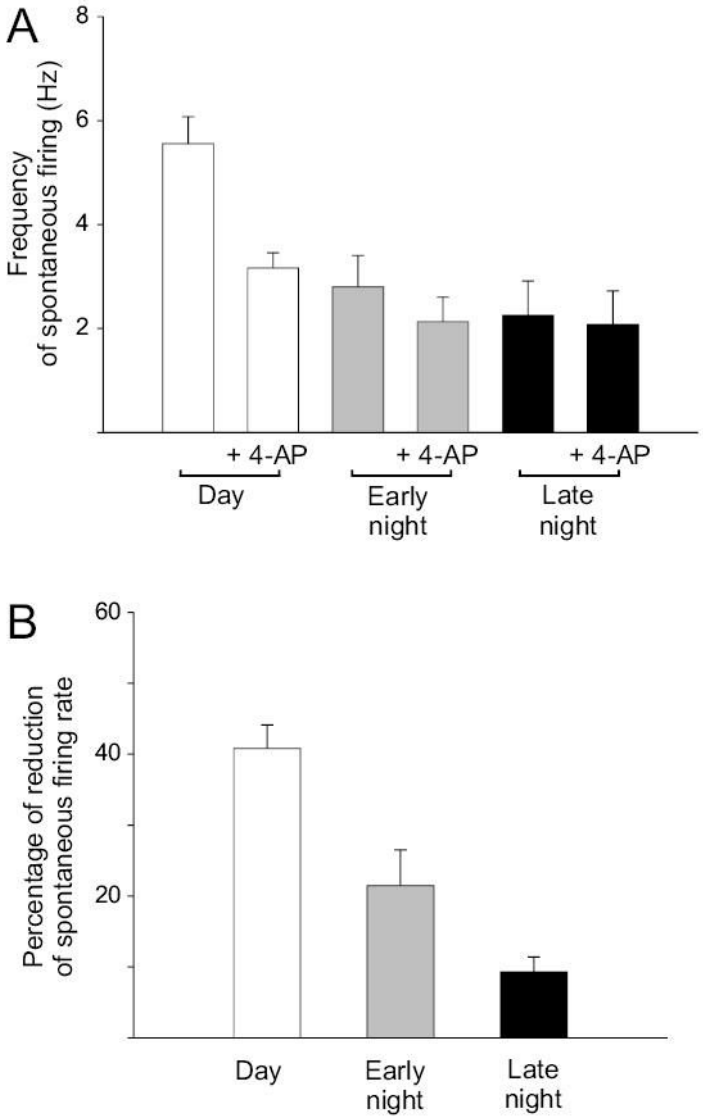

Fig. 6.

Acutely blocking the fDR current causes significant reduction in firing rate of SCN neurons during the day. (**a**) Effect of blocking fDR channels with 0.5 mM 4-AP during the day, early night, and late night in the dSCN. Similar results were obtained with application of 1 mM TEA (data not shown). (**b**) Blocking fDR channels during the day results in a significantly greater decrease in SFR compared to early and late night.

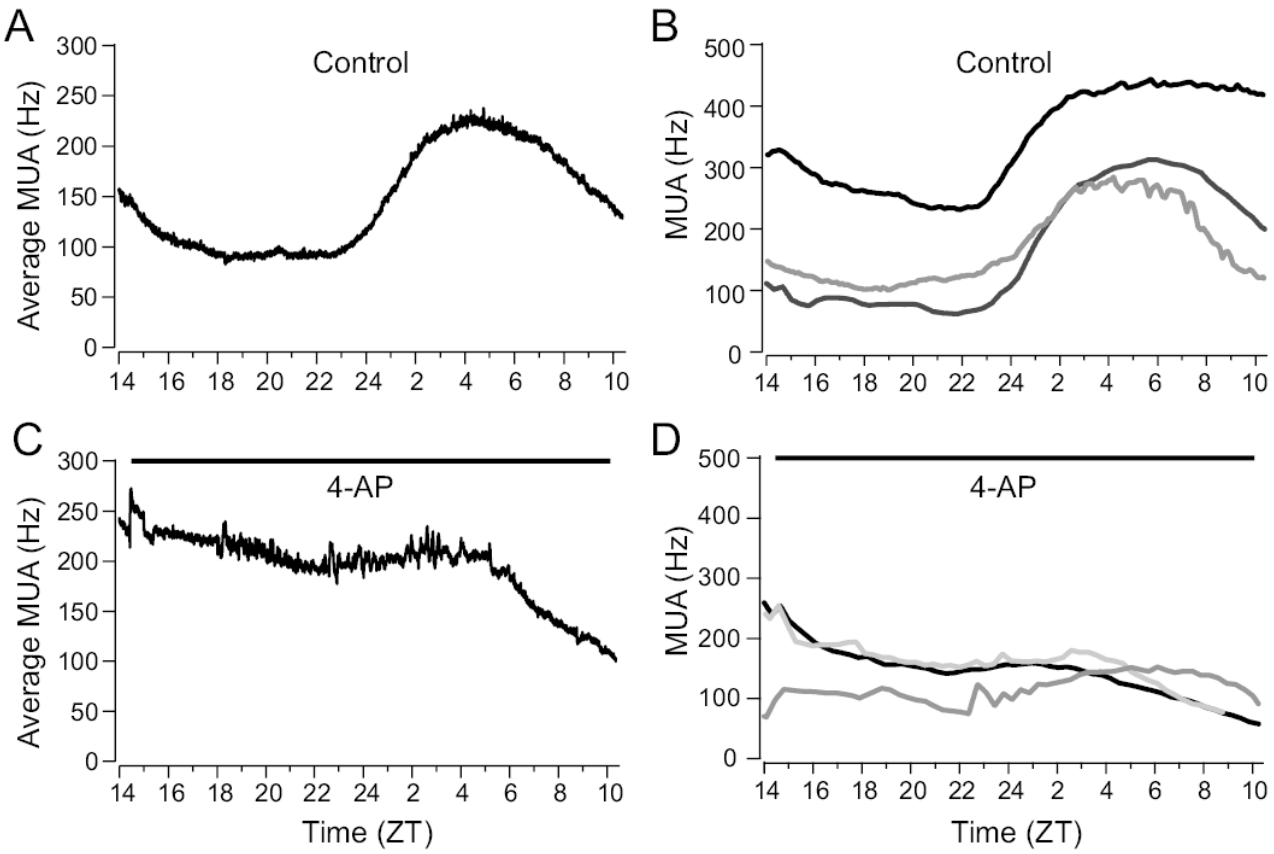

Fig. 7.

The daily rhythm in SFR is lost when the fDR current is blocked. Rhythms in multi–unit activity were recorded in mouse SCN. (**a**) Control slices (n = 6) exhibit an average circadian rhythm in spontaneous electrical activity with peak activity during the mid of the projected light phase (mid-subjective day) and low activity during the projected dark phase (mid-subjective night). (**b**) Representive examples of electrical activity recorded from 3 control SCN slices. (**c**) In contrast, this rhythm was greatly reduced or eliminated in those slices treated with 4-AP (0.5 mM, n = 6). (**d**) Representative examples of electrical activity recorded from 3 SCN slices treated with 4-AP.